

Temporal Variation of the Geopotential: Processes and Interactions Among the Earth's Subsystems

J. O. Dickey, D. Dong and R. S. Gross

Jet Propulsion Laboratory, 4800 Oak Grove Drive, Pasadena, CA 91109-8099
tel 818-354-3235; fax: 818-393-6890; e-mail: jod@logos.jpl.nasa.gov

Abstract

Seasonal variations in the Earth's gravitational field are investigated through the analysis of LAGEOS I satellite laser ranging measurements and are compared with those produced by atmospheric mass redistribution as inferred from global surface pressure data from the National Centers for Environmental Prediction (NCEP) reanalyses. The effect of oceanic tides and groundwater are considered as well. Focusing on the even zonal harmonics, atmospheric pressure fluctuations and ground water are shown to be the dominant cause of the observed zonal gravitational field variation at the annual period. At the semi-annual period, the modeled effect of the self-consistent equilibrium ocean tide dominates. The geographical distribution of the seasonal atmospheric variations are addressed. The potential use of LAGEOS for studies of polar ice sheet variation and the need for good atmospheric pressure data in this region are stressed.

Introduction

The Earth is a complex system with dynamical subsystems (such as the overlying fluid hydrosphere and atmosphere, underlying metallic core, and mantle) with complicated interactions among them (such as the melting of glaciers, sea level rise, and post-glacial rebound). Changes in the inertia tensor of the solid Earth are brought about by inter-racial stresses, the gravitational attractions associated with astronomical objects and mass redistributions in the Earth's fluid and solid region. As the Earth's gravitational field changes only in response to net mass redistribution, observations and analysis of the Earth's time varying global gravitational field permits the isolation and study of the changing mass distributions and provides insight into the processes that cause them (for a review, see *Nerem et al.*, 1995 and NRC, 1997).

Data and Analyses Procedures

LAGEOS I laser ranging measurements during 1980- 1994 are analyzed utilizing the GEODYN software package to perform numerical integration of satellite orbits and to construct normal matrices for every monthly orbit segment. We follow the procedure described in detail in *Dong et al.*, 1996 with the exception that the SPACE94 Earth Orientation Series [Gross, 1996] is used. Figure 1a shows the recovered gravitational

field coefficient ΔC_{even} (the linear combination of even zonal Stokes coefficients with each term as a function of time).

For atmospheric pressure loading we calculate the spherical harmonic coefficients of the NCEP (National Centers for Environmental Prediction) reanalysis (*Kalnay et al.*, 1996) gridded (2.5°x2.50) global surface pressure data, spanning 1980-1994 at 6-hour intervals, under both the non-inverted barometer (NIB) and inverted barometer (IB) assumptions for the response of the oceans to atmospheric pressure variations. The benefits of utilizing reanalyses results are several; the use of a single atmospheric model and the more complete edited data (as opposed to those that conform to the normal operational constraints) permit a more robust analysis. Monthly mean values of each pressure harmonic coefficient series were formed over the same time intervals as the monthly LAGEOS solutions. Individual Stokes coefficients predicted from atmospheric pressure were computed using Equation 2 from *Dong et al.* (1996). For comparison with the observed C_{even} , the same linear combination of spherical harmonics was formed using the time-dependent linear combination coefficients. Figure 1b displays the atmospheric pressure predicted C_{even} under the IB assumption. In addition, gridded values were calculated to enable a regional analysis of both pressure amplitude and phase (the convention is given in Table 2).

A self-consistent equilibrium ocean tide model [*Ray and Cartwright*, 1994, appendix B] has been used to compute the effect on the gravitational field of the annual and semiannual ocean tides. For continental surface water we have utilized the results of *Chao and O'Connor* [1988] who have computed the effect of annual and semiannual variations in continental surface water on the zonal (through degree 4) Stokes coefficients. They considered the effects of changes in snow cover, soil moisture stored in the root zone from rainfall and snowmelt, and surface water run-off that has not yet returned to the ocean. Variations in groundwater stored below the root zone were not included due to lack of accurate global estimates of this quantity. Figure 1c shows the modeled ocean tidal and surface water effects on ΔC_{even} .

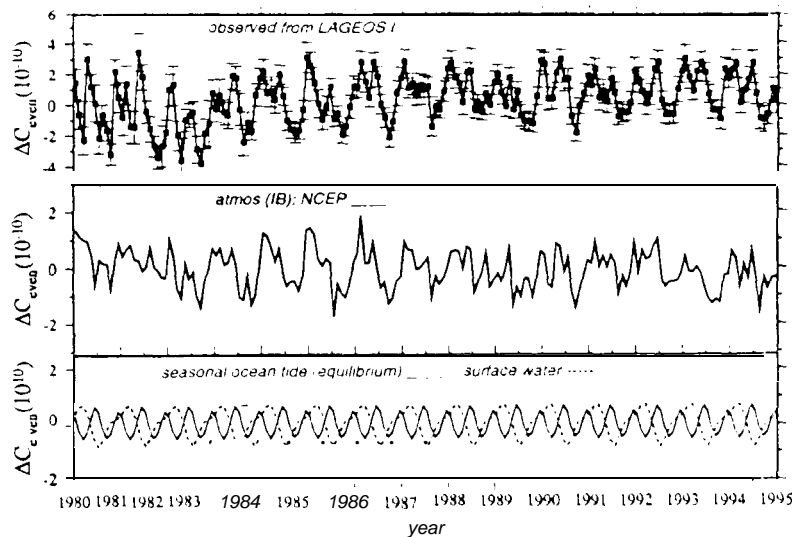


Figure 1. (a) Monthly C_{even} series spanning 1980-1994 recovered from LAGEOS I SLR data (the mean value has been removed). The error bar represents a 1σ formal uncertainty. (b) Monthly C_{even} calculated from the NCEP reanalysis (1980-1994) atmospheric surface pressure data using the same linear combination of the spherical harmonic coefficients [to which the observations are sensitive]. Solid line: NIB model; dashed line: IB model. (c) Monthly C_{even} reanalyses calculated from an equilibrium seasonal ocean tide model (solid line) and the surface water (dashed line) results of *Chao and O'Connor* [1988].

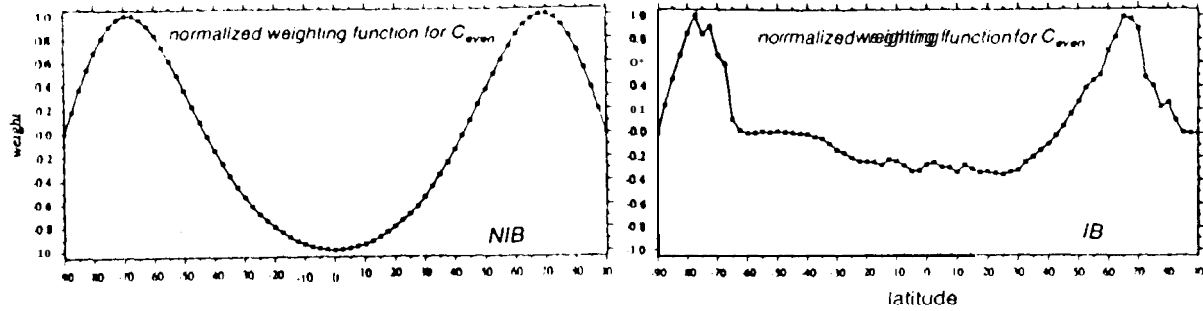


Figure 2. The normalized weighting function for C_{even} for the non-inverted barometer (NIB—left figure) and the inverted barometer (IB—right figure) case as a function of latitude.

Seasonal Global Results

The recovered monthly C_{even} solutions from the LAGEOS I data (1980-1994) are dominated by annual and semiannual variations with a significant secular trend and some indication of interannual variations (Fig. 1a). To focus on seasonal variations and the more robust results from both the NCEP and LAGEOS analyses, the observed and modeled monthly C_{even} time series from 1985 to 1994 illustrated in Figure 1 a have been highpass-filtered with a cutoff period of 2 years. Table 1 lists the correlation and variance explained between the LAGEOS-observed and predicted C_{even} series. To quantitatively compare observations with predictions at the annual and semiannual frequencies, a weighted least-squares fit for a mean, trend and sinusoidal terms at these frequencies is made to the series. The comparisons are listed in Table 2.

Comparisons from Table 1 indicate that on timescales of 1 month to 2 years, and when the atmospheric pressure effect is computed under the IB assumption, the three mechanisms together (A+O+W) can account for 78.4% of the observed variance, and have a correlation of 0.89 with the observations (note definitions in Table 1). The strong preference for the IB assumption has been shown by *Dong et al. (1996)* and is consistent with numerous studies that have demonstrated the validity of the IB assumption on these timescales.

Table 1. Correlation and Variance Explained Between Observed and Modeled C_{even} (1985-1994)

Series Considered	Inverted Barometer Assumed	
	Corr.	Var*.
At	0.83	59.0%
A + O	0.91	75.1%
A + O + W [‡]	0.89	78.4%

*The amount of the variance of the observed series explained by the modeled series is computed as: $(\sigma_o^2 - \sigma_{o-m}^2) / \sigma_o^2$ where σ_o^2 and σ_{o-m}^2 are the variance of the observed and residual (observed minus modeled) series, respectively.

^t Notations: A atmospheric pressure; O equilibrium ocean tides; W surface water.

[‡] Surface water results are from *Chao and O'Connor [1988]*.

At the annual frequency, atmospheric pressure and surface ground water effects are the dominant contributors. The best agreement with the observations is obtained when all effects (A+O+W) are considered with closure seen at the 1σ level in amplitude and at the 2σ level in phase. At the semiannual frequency, the ocean tide is the main contributor; the best agreement is obtained with the observations when only the atmospheric pressure and ocean tidal effects are considered (results are within 10 for the phase and with 20% of amplitude unaccounted for). Adding the predicted effects of surface water worsen the agreement with the observations, indicating that (a) the semiannual component of the surface water variations may not be as well determined as is the annual component, (b) other semiannual series may be erroneous, or (c) some important excitation sources are missing.

Table 2. Annual and Semiannual Variations of C_{even} from LAGEOS Observations and as Predicted from Atmospheric Pressure, Ocean Tidal, and Surface Water Fluctuations (1985-1994)

Series Considered	Annual		Semiannual	
	Amp.* (10 ⁻¹⁰)	Phase* (degrees)	Amp. (10 ⁻¹⁰)	Phase (degrees)
Observed from LAGEOS I	1.05 (0.06) [†]	26.5 (3.3)	0.93 (0.06)	116.1 (3.7)
O [#]	0.09	267.7	0.55	110.7
W [‡]	0.63	59.3	0.26	266.3
A (IB)	0.57 (0.06)	22.5 (6.3)	0.19 (0.06)	108.9 (9.6)
A (IB)+O	0.54 (0.06)	13.9 (6.7)	0.73 (0.06)	110.2 (4.9)
A (IB)+O+W	1.08 (0.06)	38.4 (3.4)	0.57 (0.06)	122.2 (7.1)

* Amplitude A and phase ϕ are defined by $A\sin[\omega(t-t_0) + \phi]$ where ω is the frequency and t_0 is January 1, 1985.

Notations are the same as Table 1.

† The quoted uncertainties given in parentheses for the LAGEOS results are the 10 formal errors in the fit. For the atmospheric series, the quoted uncertainties are the rms scatter about the fit, which are also used for the summed series since no uncertainties are available for the ocean tidal or surface water effects.

‡ From *Chao and O'Connor [1988]*.

Seasonal Regional Analysis

The global mean surface pressure (the atmosphere's moment of inertia variation) has an annual cycle of - 0.45 mbar (e.g. *Trenberth, 1981*) that is predominantly caused by seasonal variations in water vapor content, reaching its maximum in July (during Northern Hemisphere summer). Figure 3a displays the mean annual pressure amplitude under the non-inverted barometer assumption when the data from 1980-96 are considered, with Figure 3b showing the corresponding phase. The IB case (not shown) would simply have the values over the ocean replaced by a single averaged value. Several mass redistributions are clearly visible. The effects of topography, for example, over the Andes, the Tibetan Plateau, and Greenland are evident both in phase and amplitude. The

effect of distribution of land and ocean is also visible; note the high magnitude over the north Pacific and Asia, being roughly 180° out of phase. In addition, a characteristic difference exists between the northern and southern hemispheres. This seesaw is especially seen in phase and clearly visible when one examines the difference between July and January (NRC, 1997) results from the difference in the heating of the northern and southern hemispheres and the land and oceans (van den Dool and Saha, 1993). Figure 2a illustrates the sensitivity of LAGEOS I measurements of C_{even} to mass changes occurring uniformly over both land and oceans (2a) and to mass changes occurring over just land (2b). For LAGEOS I, in general, there are two areas of high sensitivity, the near polar and equatorial regions (Figure 2a). However, for mass changes over land, LAGEOS I is particularly sensitive to polar regions. Note the large sensitivity to variations south of 65° south and 50° north for Figure 2b. The semiannual terms (not shown) are roughly a factor of 3 smaller with maxima over the polar regions and the north Pacific with a complex phase structure. Applying the weighting fit (Figure 2) results in an effective C_{even} of the atmosphere that is very much dominated by the near polar regions.

The atmosphere is the Earth's best measured fluid; hence, it is critical that the best atmospheric data be available in order to unravel the effects of the Earth's other subsystems. A key issue in sea level and global change research is the rate at which Greenland and Antarctica are gaining or losing ice. Even the sign is uncertain. With accurate atmospheric pressure data and post-glacial rebound models, ice sheet mass variations can be deduced from time variable gravity measurements.

Acknowledgments

We are grateful to the Space Geodesy Branch at Goddard Space Flight Center for providing the GEODYN software and the LAGEOS normal point data, R. D. Ray for providing the self-consistent equilibrium ocean tidal admittance grid data, M. K. Cheng, R. S. Nerem, D. Rowland, M. Torrence and M. Watkins for helpful discussions. This work was performed at the Jet Propulsion Laboratory, California Institute of Technology, under contract with the National Aeronautics and Space Administration.

References

- Chao, B. F., and W. F. O'Connor, Global surface-water-induced seasonal variations in the Earth's rotation and gravitational field, *Geophys. J.*, 94, 263–270, 1988.
- Dong, D., R. S. Gross, and J. O. Dickey, Seasonal Variations of the Earth's Gravitational Field: An Analysis of Atmospheric Pressure, Ocean Tidal, and Surface Water Excitation, *Geophys. Res. Lett.*, 23, 725–728, 1996.
- Gross, R. S., et al., Combinations of Earth Orientation Series: SPACE94, COMB94, POLI94, *J. Geophys. Res.*, **101**, 8729–8740, 1996.
- Kalnay et al., The NCEP/NCAR 40-year reanalysis project, *Bull. Amer. Met. Soc.*, 77, 437–471, 1996.
- Kaula, W. M., Theory of Satellite Geodesy, 124 pp., Blaisdell, Waltham, Mass., 1966.
- NRC, Satellite Gravity and The Geosphere: Contributions to the Study of the Solid Earth and its Fluid Envelope, National Academy Press, Washington, D. C., 1997.
- Nerem, R. S., C. Jekeli, and W. M. Kaula, Gravity field determination and characteristics: Retrospective and prospective, *J. Geophys. Res.*, **100**, 15,053–15,074, 1995.
- Ray, R. D., and D. E. Cartwright, Satellite altimeter observations of the Mf and Mm ocean tides, with simultaneous orbit corrections, in *Gravimetry and Space Techniques Applied to Geodynamics and Ocean Dynamics*, edited by B. E. Schutz, A. Anderson, C. Froidevaux, and M. Parke, pp. 69–78, American Geophysical Union Geophysical Monograph 82, IUGG Volume 17, Washington, D. C., 1994.
- Trenberth, K. E., Seasonal variations in global sea level pressure and the total mass of the atmosphere, *J. Geophys. Res.*, 86, 5238–5246, 1981.
- Van den Dool, H. M., and S. Saha, Seasonal redistribution and conservation of atmospheric mass in a general circulation model, *J. Climate*, 6, 22–30, 1993.

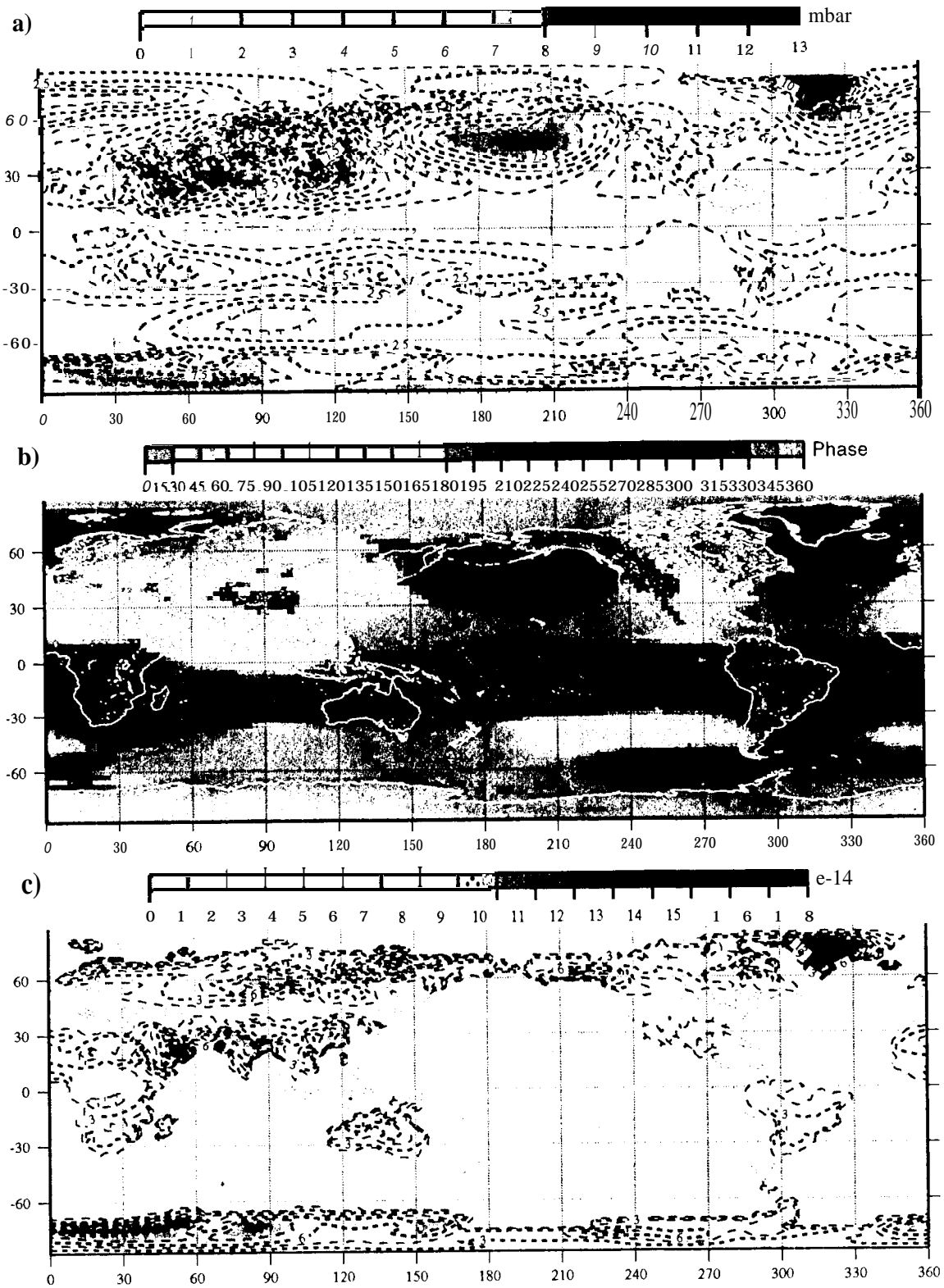


Figure 3. Annual regional pressure variation for the NIB (a) and NIB (c) case and the tori-responding phase (b and d) for the recent NCEP reanalysis (Kalnay *et al.*, 1996). The effective C_{even} annual amplitude (e),

Temporal Variation of the Geopotential: Processes and Interactions Among the Earth's Subsystems

J. O. Dickey, D. Dong and R. S. Gross
Jet Propulsion Laboratory, 4800 Oak Grove Drive, Pasadena, CA 91109-8099
tel 818-354-3235; fax: 818-393-6890; e-mail: jod @logos.jpl.nasa.gov

Abstract

Seasonal variations in the Earth's gravitational field are investigated through the analysis of LAGEOS I satellite laser ranging measurements and are compared with those produced by atmospheric mass redistribution as inferred from global surface pressure data from the National Centers for Environmental Prediction (NCEP) reanalyses. The effect of oceanic tides and groundwater arc considered as well. Focusing on the even zonal harmonics, atmospheric pressure fluctuations and ground water are shown to be the dominant cause of the observed zonal gravitational field variation at the annual period. At the semi-annual period, the modeled effect of the self-consistent equilibrium ocean tide dominates. The geographical distribution of the seasonal atmospheric variations are addressed, The potential use of LAGEOS for studies of polar ice sheet variation and the need for good atmospheric pressure data in this region are stressed.

Introduction

The Earth is a complex system with dynamical subsystems (such as the overlying fluid hydrosphere and atmosphere, underlying metallic core, and mantle) with complicated interactions among them (such as the melting of glaciers, sea level rise, and post-glacial rebound). Changes in the inertia tensor of the solid Earth are brought about by inter-racial stresses, the gravitational attractions associated with astronomical objects and mass redistributions in the Earth's fluid and solid region. As the Earth's gravitational field changes only in response to net mass redistribution, observations and analysis of the Earth's time varying global gravitational field permits the isolation and study of the changing mass distributions and provides insight into the processes that cause them (for a review, see *Nerem et al.*, 1995 and NRC, 1997).

Data and Analyses Procedures

LAGEOS I laser ranging measurements during 1980-1994 arc analyzed utilizing the GEODYN software package to perform numerical integration of satellite orbits and to construct normal matrices for every monthly orbit segment. We follow the procedure described in detail in *Dong et al.*, 1996 with the exception that the SPACE94 Earth Orientation Series [*Gross*, 1996] is used. Figure I a shows the recovered gravitational

field coefficient ΔC_{even} (the linear combination of even zonal Stokes coefficients with each term as a function of time).

For atmospheric pressure loading we calculate the spherical harmonic coefficients of the NCEP (National Centers for Environmental Prediction) reanalysis (Kalnay *et al.*, 1996) gridded ($2.5^\circ \times 2.5^\circ$) global surface pressure data, spanning 1980-1994 at 6-hour intervals, under both the non-inverted barometer (NIB) and inverted barometer (IB) assumptions for the response of the oceans to atmospheric pressure variations. The benefits of utilizing reanalyses results are several; the use of a single atmospheric model and the more complete edited data (as opposed to those that conform to the normal operational constraints) permit a more robust analysis. Monthly mean values of each pressure harmonic coefficient series were formed over the same time intervals as the monthly LAGEOS solutions. Individual Stokes coefficients predicted from atmospheric pressure were computed using Equation 2 from Dong *et al.* (1996). For comparison with the observed C_{even} , the same linear combination of spherical harmonics was formed using the time-dependent linear combination coefficients. Figure 1b displays the atmospheric pressure predicted C_{even} under the IB assumption. In addition, gridded values were calculated to enable a regional analysis of both pressure amplitude and phase (the convention is given in Table 2).

A self-consistent equilibrium ocean tide model [Ray and Cartwright, 1994, appendix B] has been used to compute the effect on the gravitational field of the annual and semiannual ocean tides. For continental surface water we have utilized the results of Chao and O'Connor [1988] who have computed the effect of annual and semiannual variations in continental surface water on the zonal (through degree 4) Stokes coefficients. They considered the effects of changes in snow cover, soil moisture stored in the root zone from rainfall and snowmelt, and surface water run-off that has not yet returned to the ocean. Variations in groundwater stored below the root zone were not included due to lack of accurate global estimates of this quantity. Figure 1c shows the modeled ocean tidal and surface water effects on ΔC_{even} .

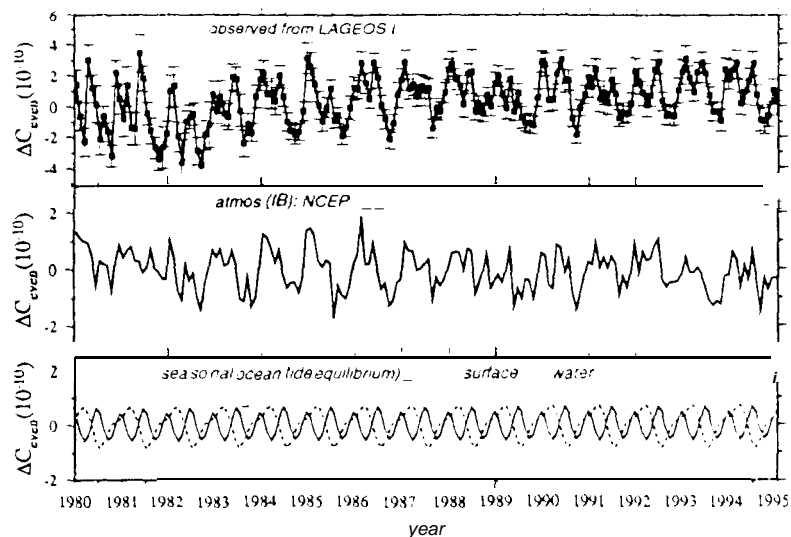


Figure 1. (a) Monthly C_{even} series spanning 1980-1994 recovered from LAGEOS I SLR data (the mean value has been removed). The error bar represents 1σ formal uncertainty. (b) Monthly C_{even} calculated from the NCEP reanalysis (1980-1994) atmospheric surface pressure data using the same linear combination of the spherical harmonic coefficients to which the observations are sensitive. Solid line: NIB model; dashed line: IB model. (c) Monthly C_{even} reanalyses calculated from an equilibrium seasonal ocean tide model (solid line) and the surface water (dashed line) results of Chao and O'Connor [1988].

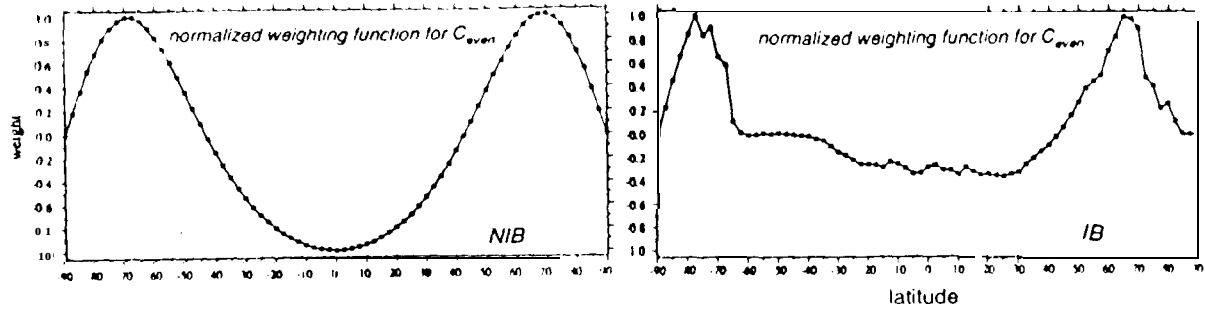


Figure 2. The normalized weighting function for C_{even} for the non-inverted barometer (NIB—left figure) and the inverted barometer (IB—right figure) case as a function of latitude.

Seasonal Global Results

The recovered monthly C_{even} solutions from the LAGEOS I data (1980-1994) are dominated by annual and semiannual variations with a significant secular trend and some indication of interannual variations (Fig. 1a). To focus on seasonal variations and the more robust results from both the NCEP and LAGEOS analyses, the observed and modeled monthly C_{even} time series from 1985 to 1994 illustrated in Figure 1 a have been highpass-filtered with a cutoff period of 2 years. Table 1 lists the correlation and variance explained between the LAGEOS-observed and predicted C_{even} series. To quantitatively compare observations with predictions at the annual and semiannual frequencies, a weighted least-squares fit for a mean, trend and sinusoidal terms at these frequencies is made to the series. The comparisons are listed in Table 2.

Comparisons from Table 1 indicate that on timescales of 1 month to 2 years, and when the atmospheric pressure effect is computed under the IB assumption, the three mechanisms together (A+O+W) can account for 78.4% of the observed variance, and have a correlation of 0.89 with the observations (note definitions in Table 1). The strong preference for the IB assumption has been shown by *Dong et al. (1996)* and is consistent with numerous studies that have demonstrated the validity of the IB assumption on these timescales.

Table 1. Correlation and Variance Explained Between Observed and Modeled C_{even} (1985-1994)

Series Considered	Inverted Barometer Assumed	
	Corr.	Var*.
A [†]	0.83	59.0%
A + O	0.91	75.1%
A + O + W [‡]	0.89	78.4%

*The amount of the variance of the observed series explained by the modeled series is computed as: $(\sigma_o^2 - \sigma_{o-m}^2) / \sigma_o^2$ where σ_o^2 and σ_{o-m}^2 are the variance of the observed and residual (observed minus modeled) series, respectively.

[†] Notations: A atmospheric pressure; O equilibrium ocean tides; W surface water.

[‡] Surface water results are from *Chao and O'Connor [1988]*.

At the annual frequency, atmospheric pressure and surface ground water effects are the dominant contributors. The best agreement with the observations is obtained when all effects (A+O+W) are considered with closure seen at the 1σ level in amplitude and at the 2σ level in phase. At the semiannual frequency, the ocean tide is the main contributor; the best agreement is obtained with the observations when only the atmospheric pressure and ocean tidal effects are considered (results are within 1σ for the phase and with 20% of amplitude unaccounted for). Adding the predicted effects of surface water worsen the agreement with the observations, indicating that (a) the semiannual component of the surface water variations may not be as well determined as is the annual component, (b) other semiannual series may be erroneous, or (c) some important excitation sources are missing.

Table 2. Annual and Semiannual Variations of C_{even} from LAGEOS Observations and as Predicted from Atmospheric Pressure, Ocean Tidal, and Surface Water Fluctuations (1985-1994)

Series Considered	Annual		Semiannual	
	Amp.* (10^{-10})	Phase* (degrees)	Amp. (10^{-10})	Phase (degrees)
Observed from LAGEOS I	1.05 (0.06) [†]	26.5 (3.3)	0.93 (0.06)	116.1 (3.7)
O [#]	0.09	267.7	0.55	110.7
W [‡]	0.63	59.3	0.26	266.3
A (: B)	0.57 (0.06)	22.5 (6.3)	0.19 (0.06)	108.9 (9.6)
A (: B)+O	0.54 (0.06)	13.9 (6.7)	0.73 (0.06)	110.2 (4.9)
A (IB)+O+W	1.08 (0.06)	38.4 (3.4)	0.57 (0.06)	122.2 (7.1)

* Amplitude A and phase ϕ are defined by $A\sin[\omega(t-t_0) + \phi]$ where ω is the frequency and t_0 is January 1, 1985.

Notations are the same as Table 1.

† The quoted uncertainties given in parentheses for the LAGEOS results are the 10 formal errors in the fit. For the atmospheric series, the quoted uncertainties are the rms scatter about the fit, which are also used for the summed series since no uncertainties are available for the ocean tidal or surface water effects.

‡ From *Chao and O'Connor* [1988].

Seasonal Regional Analysis

The global mean surface pressure (the atmosphere's moment of inertia variation) has an annual cycle of -0.45 mbar (e.g. *Trenberth, 1981*) that is predominantly caused by seasonal variations in water vapor content, reaching its maximum in July (during Northern Hemisphere summer). Figure 3a displays the mean annual pressure amplitude under the non-inverted barometer assumption when the data from 1980-96 are considered, with Figure 3b showing the corresponding phase. The IB case (not shown) would simply have the values over the ocean replaced by a single averaged value. Several mass redistributions are clearly visible. The effects of topography, for example, over the Andes, the Tibetan Plateau, and Greenland are evident both in phase and amplitude. The

effect of distribution of land and ocean is also visible; note the high magnitude over the north Pacific and Asia, being roughly 180° out of phase. In addition, a characteristic difference exists between the northern and southern hemispheres. This seesaw is especially seen in phase and clearly visible when one examines the difference between July and January (NRC, 1997) results from the difference in the heating of the northern and southern hemispheres and the land and oceans (van den Dool and Saha, 1993). Figure 2a illustrates the sensitivity of LAGEOS 1 measurements of C_{even} to mass changes occurring uniformly over both land and oceans (2a) and to mass changes occurring over just land (2b). For LAGEOS I, in general, there are two areas of high sensitivity, the near polar and equatorial regions (Figure 2a). However, for mass changes over land, LAGEOS I is particularly sensitive to polar regions. Note the large sensitivity to variations south of 65° south and 50° north for Figure 2b. The semiannual terms (not shown) are roughly a factor of 3 smaller with maxima over the polar regions and the north Pacific with a complex phase structure. Applying the weighting fit (Figure 2) results in an effective C_{even} of the atmosphere that is very much dominated by the near polar regions.

The atmosphere is the Earth's best measured fluid; hence, it is critical that the best atmospheric data be available in order to unravel the effects of the Earth's other subsystems. A key issue in sea level and global change research is the rate at which Greenland and Antarctica are gaining or losing ice. Even the sign is uncertain. With accurate atmospheric pressure data and post-glacial rebound models, ice sheet mass variations can be deduced from time variable gravity measurements.

Acknowledgments

We are grateful to the Space Geodesy Branch at Goddard Space Flight Center for providing the GEODYN software and the LAGEOS normal point data, R. D. Ray for providing the self-consistent equilibrium ocean tidal admittance grid data, M. K. Cheng, R. S. Nerem, D. Rowland, M. Torrence and M. Watkins for helpful discussions. This work was performed at the Jet Propulsion Laboratory, California Institute of Technology, under contract with the National Aeronautics and Space Administration.

References

- Chao, B. F., and W. P. O'Connor, Global surface-water-induced seasonal variations in the Earth's rotation and gravitational field, *Geophys. J.*, 94, 263–270, 1988.
- Dong, D., R. S. Gross, and J. O. Dickey, Seasonal Variations of the Earth's Gravitational Field: An Analysis of Atmospheric Pressure, Ocean Tidal, and Surface Water Excitation, *Geophys. Res. Lett.*, 23, 725–728, 1996.
- Gross, R. S., et al., Combinations of Earth Orientation Series: SPACE94, COMB94, POL94, *J. Geophys. Res.*, 101, 8729–8740, 1996.
- Kalnay et al., The NCEP/NCAR 40-year reanalysis project, *Bull. Amer. Met. Soc.*, 77, 437–471, 1996.
- Kaula, W. M., Theory of Satellite Geodesy, 124 pp., Blaisdell, Waltham, Mass., 1966.
- NRC, Satellite Gravity and The Geosphere: Contributions to the Study of the Solid Earth and its Fluid Envelope, National Academy Press, Washington, D. C., 1997.
- Nerem, R. S., C. Jekeli, and W. M. Kaula, Gravity field determination and characteristics: Retrospective and prospective, *J. Geophys. Res.*, 100, 15,053–15,074, 1995.
- Ray, R. D., and D. E. Cartwright, Satellite altimeter observations of the M_f and M_{rn} ocean tides, with simultaneous orbit corrections, in *Gravimetry and Space Techniques Applied to Geodynamics and Ocean Dynamics*, edited by E. E. Schutz, A. Anderson, C. Froidevaux, and M. Parke, pp. 69–78, American Geophysical Union Geophysical Monograph 82, IUGG Volume 17, Washington, D. C., 1994.
- Trenberth, K. E., Seasonal variations in global sea level pressure and the total mass of the atmosphere, *J. Geophys. Res.*, 86, 5238–5246, 1981.
- Van den Dool, H. M., and S. Saha, Seasonal redistribution and conservation of atmospheric mass in a general circulation model, *J. Climate*, 6, 22–30, 1993.

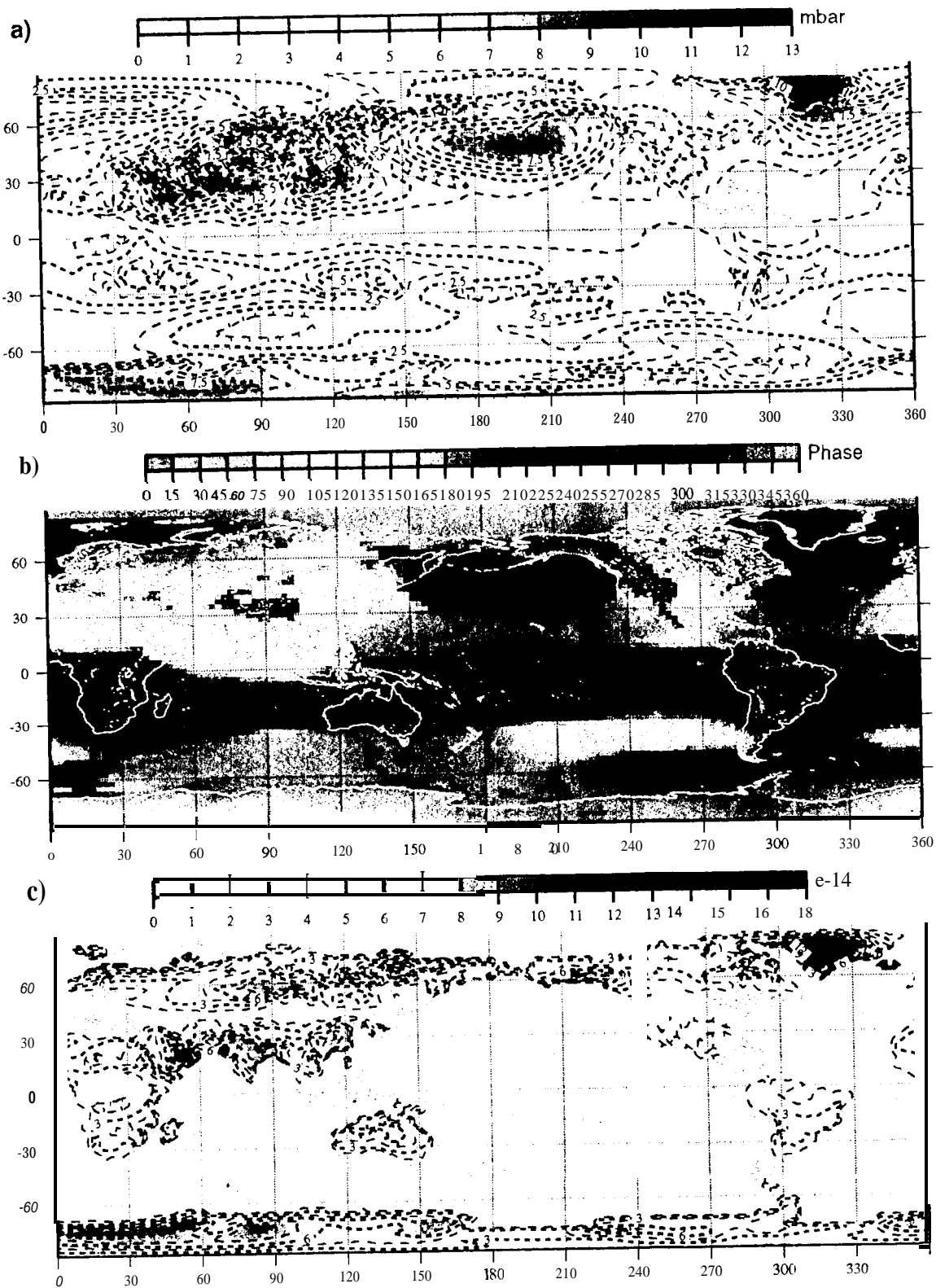


Figure 3. Annual regional pressure variation for the NIB (a) and NIB (c) case and the corresponding phase (b and d) for the recent NCEP reanalysis (Kalnay et al., 1996). The effective C_{even} annual amplitude (e).